CONTROL STRATEGIES FOR A SPARK IGNITION ENGINE DURING THE WARM-UP PHASE

Maria Carmela De Gennaro*, Giovanni Fiengo*, Luigi Glielmo* and Stefania Santini†

* Dipartimento di Ingegneria, Università degli studi del Sannio, Benevento, email: {degennaro,gifiengo,glielmo}@unisannio.it
† Dipartimento di Informatica e Sistemistica, Università degli Studi di Napoli Federico II, email: stsantin@unina.it

Keywords: Automotive control, Emission control, Warm-up control, Internal combustion engine, Vehicles and transportation system

Abstract

Atmospheric pollution is an open problem that hits above all the cities. It is caused by different factors, as exhaust gas of the cars. To limit the emission level a three way catalytic converter is used to post-treat exhaust gases produced by combustion. The catalyst efficiency depends on the operating point; particularly during the warm-up phase the largest amount of pollutants is produced because the catalyst is not properly working. An appropriate control strategy is necessary during this phase in order to minimize dangerous emissions. In this paper, different innovative control strategies, designed for the warm-up phase, are presented. Firstly a simple controller, based on PI regulator, is compared with a more complex controller realized using the LQ technique. Finally, a secondary air injection on the exhaust manifold is considered and the two control strategies are implemented with this new control input.

Regular paper.

1 Introduction

Combustion in a Spark Ignition Internal Combustion Engine (SI-ICE) causes the production of pollutants, mainly nitrogen oxides, $\mathrm{NO_x}$, carbon monoxide, CO, and unburned hydrocarbons, HC. Since 1971 the European Community imposed limits for the pollutants production, which are periodically let down to try to reduce the atmospheric pollution. In current technology vehicles, a Three Way Catalytic Converter (TWC) placed on the exhaust manifold, is used to reduce pollutant emissions. The TWC efficiency depends on the operation point, such as device temperature and air-fuel ratio in the feedgas. The conversion efficiency is more than 98% only for warmed-up catalysts and in presence of stoichiometric air-fuel ratio. Obviously these conditions can be not achieved at the engine cold-start and TWC transient thermal phase. New restrictions imposed on emissions require the design of new control strategies. An innovative warm-up control system, not yet available on commercial cars, has to guarantee:

- an earlier activation of the TWC;
- air-fuel ratio regulation around the stoichiometric value;
- the tracking of an assigned torque profile, to guarantee the engine performances.

To reach the impose requirements, different model based warm-up control strategies are designed. To this aim, an improved version of ICE and TWC models presented in [1] are used. In the following the ICE model is briefly described pointing out the improvements. Then two control strategies aimed to minimize pollutant emission are shown. Finally a new control system working on a secondary air injection in the exhaust manifold is presented. By using this new actuation it is possible to reach higher performances of the whole system. All the proposed strategies are compared by simulations on real data.

2 Plant Model

The design of new real time applications, as warm-up controllers, starts from reliable mathematical models of the dynamic behavior of the SI-ICE and the catalyst. Here we present an improved version of the plant model presented in [1]. In the following we briefly introduced the ICE model highlighting all the new features. The TWC phenomenological model can be found in [1].

The scheme in Figure 1 represents a control oriented model of ICE. It describes the combustion process without including fuel and air dynamics across the manifold. System inputs are air mass flow rate $\dot{\mathrm{m}}_\mathrm{a}$, air/fuel ratio λ entering the cylinder, spark advance angle θ. Since the engine speed n is determined by the driver commanding the torque, it is considered in this model as an input. In the following, the blocks composing the whole engine model are presented.

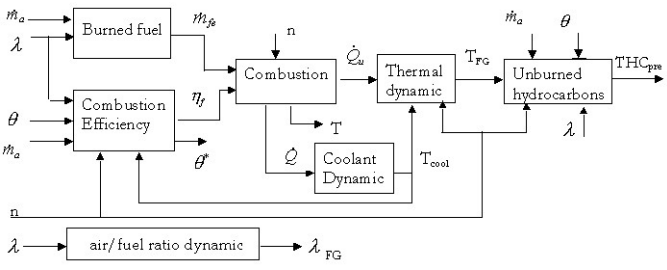

Figure 1: Engine model.

The block *Burned fuel* computes the fuel charge, $\dot{\mathrm{m}}_\mathrm{fe}$, actually burned during the combustion. Supposing that only the air-fuel

mixture that is in a stoichiometric ratio participates actively to the combustion process, if the air-fuel mixture is lean ($\lambda \geq 1$) all the fuel in the cylinder takes part at the combustion ($\dot{\mathrm{m}}_{\mathrm{fe}} = \dot{\mathrm{m}}_{\mathrm{a}}/\lambda_{\mathrm{ST}}/\lambda$); conversely, in rich condition ($\lambda < 1$), an amount of fuel equal to the 14.6-th part of the cylinder air is burned ($\dot{\mathrm{m}}_{\mathrm{fe}} = \dot{\mathrm{m}}_{\mathrm{a}}/\lambda_{\mathrm{ST}}$).

The block *Combustion efficiency* estimates the efficiency of the engine, η_f, in transforming the chemical energy of the fuel into mechanical energy through combustion. It is function of the engine operating point and the distance between the real and the nominal value of the spark advance $(\theta - \theta^*)$; θ^* is the nominal value of the spark advance for the production of the torque from the combustion (see [1] for further details).

The block *Combustion* estimates the effective torque T, generated by the combustion, as

$$\mathrm{T} = \frac{\eta_{\mathrm{f}} \dot{\mathrm{m}}_{\mathrm{fe}} \mathrm{Q}_{\mathrm{HV}}}{\mathrm{n}}, \tag{1}$$

where the quantity of energy generated by the combustion of the fuel and not transformed into effective power, $(1 - \eta_f)\dot{\mathrm{m}}_{\mathrm{fe}}\mathrm{Q}_{\mathrm{HV}}$, is dissipated as heat. A part of this thermal energy warms the engine mechanical components while the remaining part is transferred to the exhaust gas. It is supposed that the quantity of energy that is transferred to the exhaust gas is

$$\dot{\mathrm{Q}}_{\mathrm{u}} = \beta(1 - \eta_{\mathrm{f}})\dot{\mathrm{m}}_{\mathrm{fe}}\mathrm{Q}_{\mathrm{HV}}, \tag{2}$$

while the energy transferred to the coolant and the environment is

$$\dot{\mathrm{Q}} = (1 - \beta)(1 - \eta_{\mathrm{f}})\dot{\mathrm{m}}_{\mathrm{fe}}\mathrm{Q}_{\mathrm{HV}}. \tag{3}$$

The coefficient β describes the time-varying partition of thermal energy as a function of the coolant temperature, $\mathrm{T}_{\mathrm{cool}}$. During the cold start the part of the heat which goes toward the engine is approximately 75% of the total dissipated heat ; once warmed up ($\mathrm{T}_{\mathrm{cool}}$ has reached the steady state value $\mathrm{T}_{\mathrm{coolMax}}$) we assume that half of the heat is directed toward the engine and half to the exhaust gas. More precisely, β depends linearly on $\mathrm{T}_{\mathrm{cool}}$

$$\beta(\mathrm{T}_{\mathrm{cool}}) = \beta_0 + \mathrm{K}_\beta(\mathrm{T}_{\mathrm{cool}} - \mathrm{T}_{\mathrm{env}}), \tag{4}$$

where $\mathrm{K}_\beta = 0.25/(\mathrm{T}_{\mathrm{coolMax}} - \mathrm{T}_{\mathrm{env}})$, $\beta_0 = \frac{1}{4}$.

A simple phenomenological model, enclosed in *Coolant Dynamic* block, describes the engine thermal dynamic. The coolant temperature has been chosen as representative of the engine temperature behavior as

$$\dot{\mathrm{T}}_{\mathrm{cool}} = \mathrm{d}_0\dot{\mathrm{Q}} - \mathrm{d}_1(\mathrm{T}_{\mathrm{cool}} - \mathrm{T}_{\mathrm{env}}). \tag{5}$$

In our approach, we model the effect of the coolant control normally implemented on a real car, simply by inserting a saturation for the maximum value of the coolant temperature.

The block *Thermal dynamic* models the dynamical behavior of the exhaust gas temperature, T_{FG}. The inputs of this block are heat flow (equation (2)) generated by combustion, coolant temperature $\mathrm{T}_{\mathrm{cool}}$, and engine speed n:

$$\dot{\mathrm{T}}_{\mathrm{FG}} = \mathrm{a}_0\dot{\mathrm{Q}}_{\mathrm{u}} - \mathrm{a}_1\mathrm{n}(\mathrm{T}_{\mathrm{FG}} - \mathrm{T}_{\mathrm{cool}}). \tag{6}$$

The unburned hydrocarbons THC are calculated, in the rightmost block, as a function of the feedgas temperature T_{FG}, air mass flow rate $\dot{\mathrm{m}}_{\mathrm{a}}$, spark advance θ, engine speed n and air/fuel ratio λ, through a black box model (see [1] for further details).

The *air/fuel ratio dynamic* is described by taking into account both combustion and transport delay

$$\lambda_{\mathrm{FG}}(t) = \lambda(t - \delta) + n(t) + d(t), \tag{7}$$

where λ_{FG} is the feedgas air/fuel ratio, δ is the total delay, $n(t)$ is the white noise with zero average, $d(t)$ mimics injection uncertainties.

All the parameters in the previous equations are identified through both classic recursive and nonlinear least square algorithms [2] .

3 Warm-Up Control

Warm-up control strategy commands the engine in order to minimize the polluting emissions at the TWC outlet. Here the controller mainly works on the spark advance angle, θ, to fast increase the feedgas temperature: by reducing spark advance angle, combustion efficiency decreases, consequently heat losses are higher and thus contributes to the feedgas warming. Obviously, this strategy reduces the effective produced torque and, in order to ensure driver requirement, this has to be compensated by increasing the air mass flow rate supply to cylinders (see equation (1)). The peculiar use of spark angle and air mass flow rate generates an extra-pollution, that should be compensated by earlier activation of catalytic reactions. It is so crucial to balance this two tendencies, increasing feedgas temperature vs. extra-pollution, in order to optimize the results of the control strategy so to minimize the total amount of outlet catalyst emissions. Moreover the controller also regulates the injection duration in order to guarantee a stoichiometric mixture and, thus, as well known [3], maximum TWC conversion efficiency.

All the control strategies that will be presented in the following feed back measurements of feedgas temperature, $\mathrm{T}_{\mathrm{FGm}}$, and air/fuel ratio, λ_{FGm}, (see Figure 2). Notice that air/fuel ratio measures used in this work refer to a linear pre-heated λ-sensor, (UEGO - Universal Exhaust Gas Oxygen). In the controller design, thermocouple dynamics are neglected, while a first order linear system models the UEGO sensor dynamic behavior.

Since on-line pollutants analyzer are not available on commercial cars, no feed-back loop is closed around the TWC (see Figure 2). Thus, in this work, the TWC dynamic model is only used for tuning the controller parameters and for strategies validation and comparison.

In this work, as already mentioned, we design two different systems by including or not a second air injection in the exhaust manifold. For each system, two control strategies are designed and the performances are compared. The strategies are also compared to the controller really implemented in a commercial car in order to test the effectiveness. The performances regards

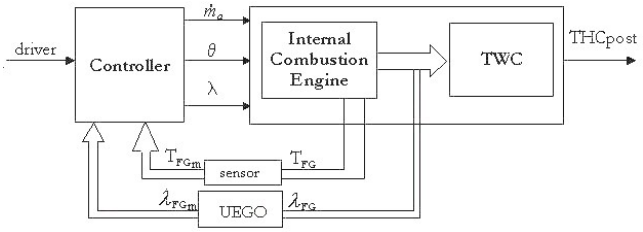

Figure 2: Control scheme.

the first 300 seconds of a standard European drive cycle (ECE, Economic Commission for Europe, cycle). Experimental data were furnished by Magneti Marelli for a Golf 1600 cc engine.

On a commercial engine, different controllers with different priorities simultaneously run in order to ensure the optimal working in all operative points. In particular idle speed control is activated when the engine speed is lower than a fixed threshold to avoid extinction. Usually idle speed control has higher priority than emission control, thus our controller is deactivated during idle and the commercial controller drives the engine. Finally, our warm-up controllers are completely deactivated once the feedgas temperature reference, a parameter to be chosen, is reached.

All the warm-up control strategies proposed in this paper work in different manners on the spark advance angle, while have the same control approach for the regulation of air mass flow rate and air/fuel ratio. In particular the air/fuel ratio controller, aimed to ensure the stoichiometric mixture, is a PI regulator with anti-wind-up scheme and a feed forward action equal to 1. The in-cylinder air mass flow rate, $\dot{\mathrm{m}}_{\mathrm{a}}$, necessary to compensate the torque reduction, is computed by a feed-forward action as follows

$$\dot{m}_a = \frac{\lambda_{\mathrm{ST}} \mathrm{n} \mathrm{T}_{\mathrm{rif}}}{\eta_{\mathrm{f}} \mathrm{Q}_{\mathrm{HV}}} \cdot \begin{cases} \lambda & \text{when} \quad \lambda \geq 1 \\ 1 & \text{when} \quad \lambda < 1 \end{cases} \tag{8}$$

where $\mathrm{T}_{\mathrm{rif}}$ is the reference torque driven by the driver.

3.1 PI controller

This first strategy for the regulation of the spark advance is based on a simple approach. Goal of the controller is to regulate the feedgas temperature T_{FG} to an appropriate reference $\mathrm{T}_{\mathrm{FGrif}}$. To this aim the spark advance angle is determined by a PI controller, realized with anti wind-up scheme, and a feed-forward action equal to the nominal value of the spark advance angle θ^*. As already mention this action obviously deteriorate the combustion process increasing the heat production. The torque reduction is compensated by working on the air mass flow rate (eq. (8)). The PI parameters are tuned with a purposely designed genetic algorithm [4]. In Figures 3 - 4 the PI controller and the commercial controller performances are compared on the range between the 40th and the 70th second of the ECE cycle. The vertical dotted line represents the time instant when feedgas temperature reaches its reference.

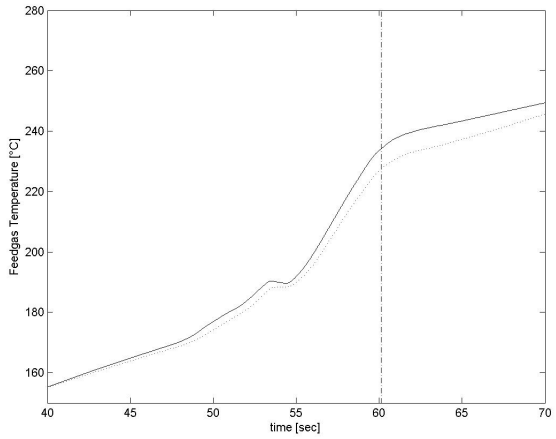

Figure 3: Feedgas temperature, T_{FG} [°C], when it is applied respectively the PI controller (solid line) and the commercial controller (dotted line).

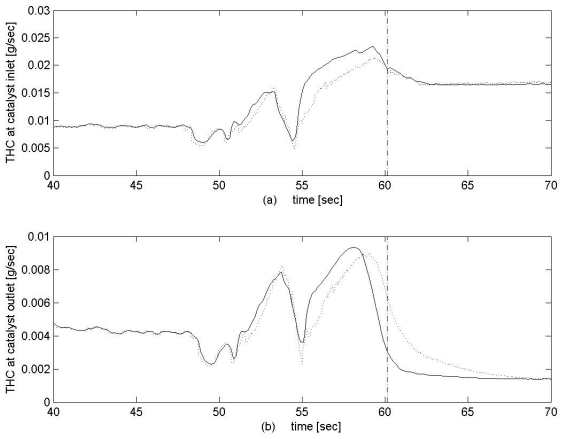

Figure 4: Total unburned hydrocarbons at catalyst inlet [g/sec], $\mathrm{THC}_{\mathrm{pre}}$ (a), and Total unburned hydrocarbons at catalyst outlet [g/sec], $\mathrm{THC}_{\mathrm{post}}$ (b), when it is applied respectively the PI controller (solid line) and the commercial controller (dotted line).

At about the 58-th second there is the biggest effort of the warm-up control in increasing the feedgas temperature (see Figure 3) corresponding to a significant increase of the unburned hydrocarbons production (see Figure 4(a)). This is efficiently compensate by the earlier activation of the catalyst (see Figure 4(b)).

Results on the amount of the Total Unburned Hydrocarbons (THC) emitted in the air is reported in table 1: with respect to the commercial controller, a THC increase of 0.72% at catalyst inlet and a THC decrease of 1.41% at the catalyst outlet can be noted.

3.2 LQ controller

The LQ warm-up controller improves the results obtained with PI regulator. Details on the whole LQ warm-up technique can be found in [5]. Here we just briefly highlights that the LQ control works on a linearized version of the engine model presented in the section 2, aimed to optimize the following cost function

$$V = \frac{1}{2}\int[(\mathrm{T_{FG}} - \mathrm{T_{FGrif}})^2\mathrm{Q} + (\theta - \theta^*)^2\mathrm{R}]\mathrm{dt}, \qquad (9)$$

where Q and R are the weight matrices. The control input is computed as

$$\theta_{\mathrm{opt}} = -\mathrm{R}^{-1}\mathrm{B}^{\mathrm{T}}\mathrm{P}\delta\mathrm{T_{FG}} - \mathrm{R}^{-1}\mathrm{B}^{\mathrm{T}}\mathrm{b} + \theta^*, \qquad (10)$$

where P is obtained solving the algebraic Riccati equation; B is the input matrix in the linearized model; $\delta\mathrm{T_{FG}}$ is the distance between current feedgas temperature and linearization point; the controller parameters are tuned with a genetic algorithm. In the following figures a comparison between LQ strategy and with the commercial controller is shown .

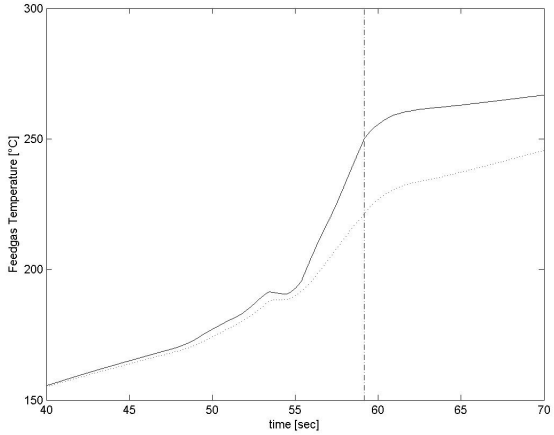

Figure 5: $\mathrm{T_{FG}}$ [°C], when it is applied respectively the LQ controller (solid line) and the commercial controller (dotted line).

In the Table 1 is shown a numeric comparison of the engine performances, when it is equipped respectively by LQ, PI and commercial controller. With the LQ controller there is an 0.44% increase of THC at catalyst inlet, and a 4.37% decrease of THC at the catalyst outlet.

	LQ	PI	Com.	LQ	PI
$\int THC_{pre}$	3.441g	3.451g	3.426g	0.44%	0.72%
$\int THC_{post}$	0.678g	0.699g	0.709g	-4.37%	-1.41%

Table 1: Comparison between LQ, PI and commercial (Com.) controller. Percentage values refer to variation from the commercial controller performances.

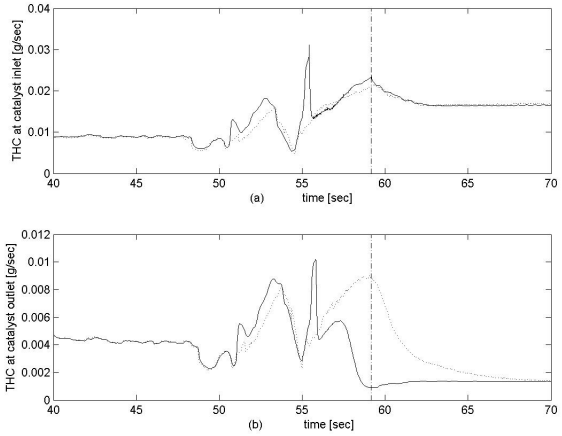

Figure 6: $\mathrm{THC_{pre}}$ (a), and $\mathrm{THC_{post}}$ (b), when it is applied respectively the LQ controller (solid line) and the commercial controller (dotted line).

3.3 Secondary air injection modelling

To investigate about the possibility of an improvement in the results of the previous strategies, here we suppose to arrange a secondary air injection, $\dot{\mathrm{m}}_{\mathrm{a2}}$, in the exhaust manifold. This injection could cause another combustion in the exhaust manifold, producing two useful effects for the warm-up phase:

- the reduction of THC as input of the catalyst;
- a faster increase of the feedgas temperature, due to the heat produced by second combustion, entirely given to the feedgas.

Since we do not have experimental data referring to this plant, we make same reasonable hypothesis in order to develop a model for this new system:

1. the secondary air injection is used only during the warm-up phase;
2. the secondary combustion could only happen if the mixture temperature is sufficiently high (we suppose a threshold of 150°C).
3. if, during the second combustion, the mixture is lean, burns the 50% of THC in the feedgas, otherwise burns the 50% of the THC that are in a stoichiometric fraction with $\dot{\mathrm{m}}_{\mathrm{a2}}$.
4. the secondary combustion happens with a probability of 70%.

In Figure 7 is shown the secondary combustion block.

The inputs are air/fuel ratio in the feedgas (λ_{FG}), first and second air mass flow rate ($\dot{\mathrm{m}}_{\mathrm{a}}$ and $\dot{\mathrm{m}}_{a2}$), feedgas temperature ($\mathrm{T_{FG}}$) and unburned hydrocarbons in the feedgas (THC).

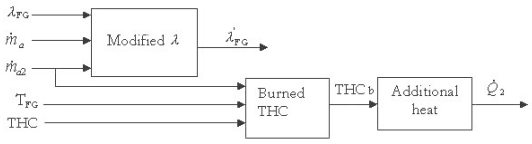

Figure 7: Secondary combustion model.

The block *Modified* λ computes the new value for air/fuel ratio, λ'_{FG}, due to the secondary air mass flow:

$$\lambda'_{\mathrm{FG}} = \frac{\dot{\mathrm{m}}_{\mathrm{a}} + \dot{\mathrm{m}}_{\mathrm{a2}}}{(\dot{\mathrm{m}}_{\mathrm{a}}/\lambda_{\mathrm{FG}})} \tag{11}$$

The block *Burned THC* computes the hydrocarbons that are burned for the secondary combustion, $\mathrm{THC_b}$:

$$\mathrm{THC_b} = \frac{1}{2}\frac{\dot{\mathrm{m}}_{\mathrm{a2}}}{\lambda_{\mathrm{ST}}} \cdot \begin{cases} \dfrac{1}{\lambda'_{\mathrm{FG}}} & \lambda'_{\mathrm{FG}} \geq 1 \\ 1 & \lambda'_{\mathrm{FG}} < 1 \end{cases} \qquad \mathrm{T_{FG}} > 150^{\circ}\mathrm{C}. \tag{12}$$

The block *Additional heat* computes the heat $\dot{\mathrm{Q}}_2$ produced by the secondary combustion:

$$\dot{\mathrm{Q}}_2 = \mathrm{Q_{HV}} \cdot \mathrm{THC_b}. \tag{13}$$

This heat warms the feedgas, thus equation (6) can be modified as

$$\dot{\mathrm{T}}_{\mathrm{FG}} = \mathrm{a_0}\dot{\mathrm{Q}}_{\mathrm{u}} - \mathrm{a_1 n}(\mathrm{T_{FG}} - \mathrm{T_{cool}}) + \mathrm{a_2}\dot{\mathrm{Q}}_2. \tag{14}$$

The new engine model is used in a feedback control system, as shown in Figure 8.

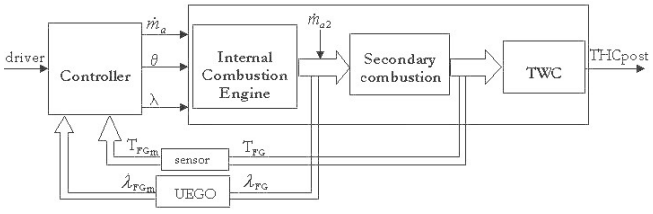

Figure 8: Control scheme with the secondary air injection.

As before, we compare the performances of two different controllers which work on the spark advance angle θ (PI and LQ controllers). The on-line available measurements are feedgas temperature ($\mathrm{T_{FG}}$) after the secondary combustion and air-fuel ratio in the feedgas before the secondary combustion. The feed-forward action for the second air injection is computed as a fraction of $\dot{\mathrm{m}}_{\mathrm{a}}$

$$\dot{\mathrm{m}}_{\mathrm{a2}} = \frac{\dot{\mathrm{m}}_{\mathrm{a}}}{80}. \tag{15}$$

The controllers parameters are again tuned with purposely designed genetic algorithm. As before, in the idle speed phase the engine is driven by the commercial controller and the warm-up controller is definitely deactivate when the feedgas temperature has reached its reference.

3.4 PI controller with secondary injection

This control strategy is simply obtained combining the controller described in section 3.1 and a feed-forward action that computes the air mass flow rate to be injected in the exhaust manifold (see eq. 15). In particular, the spark advance angle and the air/fuel ratio are calculated with a PI regulator realized with an anti wind-up scheme, aimed to control respectively the feedgas temperature and the air/fuel ratio of the mixture. The air mass flow rate inside the cylinder is, once more, determined to compensate the torque reduction, as described in equation 8. In Figures 9 - 10, a comparison between this control strategy and the commercial controller is shown, on the range between 30 and 70 seconds.

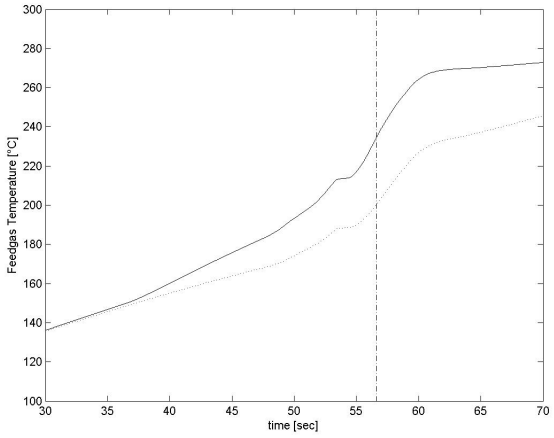

Figure 9: $\mathrm{T_{FG}}$ [°C], when it is applied respectively the PI controller with secondary injection (solid line) and the commercial controller(dotted line).

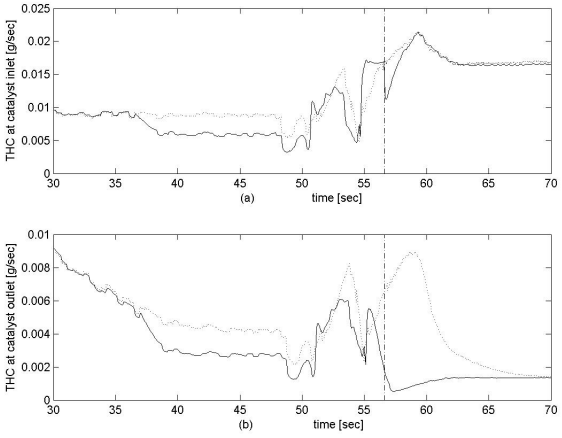

Figure 10: $\mathrm{THC_{pre}}$ (a), and $\mathrm{THC_{post}}$ (b), when it is applied respectively the PI controller with secondary injection (solid line) and the commercial controller (dotted line).

At about the 37-th second, the feedgas temperature $\mathrm{T_{FG}}$

reaches the threshold value for the combustion in the exhaust manifold (see Figure 9), and the controller starts to inject air in the manifold. According to equation 12, the unburned hydrocarbons in the exhaust manifold burn causing an extra heat production that warms the feedgas and the catalyst quickly (see Figure 9). Moreover, as an other consequence of the second combustion, the THC at the inlet of the catalyst are reduced (see Figure 10(a)). Numerical results on the amount of THC at the outlet of the TWC, with respect to the commercial controller, shows a decrease of 0.82% at catalyst inlet and a decrease of 7.89 at catalyst outlet (see Table 2).

3.5 LQ controller with secondary injection

The LQ control strategy, purposely designed for this system configuration, improves the PI regulator performances previously described. The LQ technique is been described (see section 3.2) so as the management of the other control inputs: air/fuel ratio; air mass flow entering in the cylinder (see eq. 8); secondary air mass flow injected in the exhaust manifold (see eq. 15).

In the following figures, simulation results are plotted compared to the commercial controller performances. Finally, in Table 2 is shown a numeric comparison of the engine performances, equipped respectively by LQ, PI and commercial controller. With the LQ strategy there is an 1.58% decrease of THC at catalyst inlet, and a 9.59% decrease of THC at the catalyst outlet.

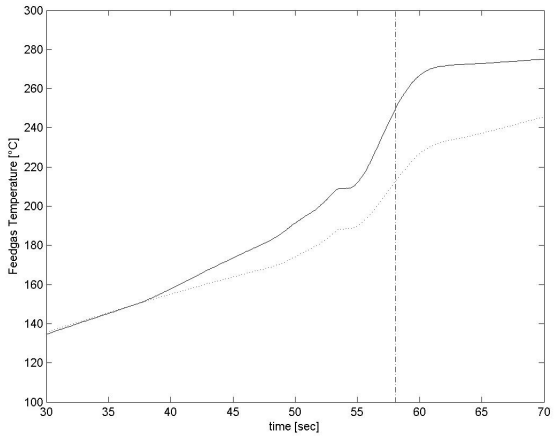

Figure 11: $\mathrm{T_{FG}}$ [°C], when it is applied respectively the LQ controller with secondary injection (solid line) and the commercial controller(dotted line).

4 Conclusion

In this paper different refinements of a warm-up control strategy for the cascade SI-ICE/TWC were presented. Future work in this research field will concern with implementation of the controllers on a vehicle.

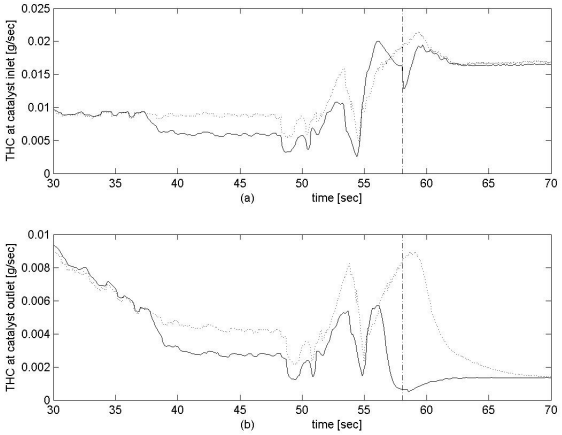

Figure 12: $\mathrm{THC_{pre}}$ (a), and $\mathrm{THC_{post}}$ (b), when it is applied respectively the LQ controller with secondary injection (solid line) and the commercial controller (dotted line).

	LQ	PI	Com.	LQ	PI
$\int THC_{pre}$	3.372g	3.398g	3.426g	-1.58%	-0.82%
$\int THC_{post}$	0.641g	0.653g	0.709g	-9.59%	-7.89%

Table 2: Comparison between LQ, PI and commercial (Com.) controller. Percentage values refer to variation from the commercial controller performances.

5 Extra Nomenclature

λ	air/fuel ratio, normalized to the stoichiometric value ([/])
λ_{ST}	stoichiometric air/fuel ratio equal to 14.6([/])
$\mathrm{Q_{HV}}$	fuel low heating value equal to 46
$\mathrm{T_{env}}$	environment temperature ([°C])

References

[1] G. Fiengo, L. Glielmo, S. Santini, and G. Serra, "Control oriented models for spark ignited engines and twc during the warm-up phase," *2002 American Control Conference*, 2002.

[2] S. Bittanti, *Identificazione dei modelli e controllo adattativo*, Pitagora Editrice, 1997.

[3] John B. Heywood, *Internal Combustion Engine Fundamentals*, McGraw-Hill International Editions-Automotive Technology Series, 1988.

[4] L. Davis, *Handbook of Genetic Algorithms*, Van Nostrand Reinhold, 1991.

[5] G. Fiengo, L. Glielmo, S. Santini, and G. Serra, "Control of the exhaust gas emissions during the warm-up process of a twc-equipped si-engine," *International Federation of Automatic Control 15th World Congress*, Barcelona, Spain, 2002.